Synthesis, Structure, and Study of the Cytotoxic Activity of Zinc(II) Complex with 5-Benzyltetrazole and 1,10-Phenanthroline

**E. A. Ermakova[a], Yu. A. Golubeva[a], K. S. Smirnova[a], L. S. Klyushova[b],
I. V. El'tsov[c], and E. V. Lider[a], ***

[a] Nikolaev Institute of Inorganic Chemistry, Siberian Branch, Russian Academy of Sciences, Novosibirsk, Russia
[b] Research Institute of Molecular Biology and Biophysics, Federal Research Center for Fundamental and Translational Medicine, Novosibirsk, Russia
[c] Novosibirsk National Research State University, Novosibirsk, Russia
*e-mail: lisalider@ngs.ru

Abstract—The complex $[Zn(Phen)(H_2O)L_2]$ (**I**), where HL is 5-benzyltetrazole, Phen is 1,10-phenanthroline, was synthesized. The compound was characterized by standard physicochemical methods (elemental analysis, powder X-ray diffraction, IR spectroscopy). According to X-ray diffraction data (CCDC no. 2220597), zinc coordination environment in the crystal structure of **I** corresponds to a distorted trigonal bipyramid. The ligand HL is monodentate and is coordinated via tetrazolate ring nitrogen. The stability of complex **I** was studied by NMR spectroscopy in DMSO. The cytotoxic properties of the compound were assessed against HepG-2 (hepatocellular carcinoma) and MRC-5 (noncancerous human fibroblasts) cells. Complex **I** exhibits weak cytotoxic properties in the studied concentration range (1−100 µM).

INTRODUCTION

Zinc is a biocompatible element present in the active sites of almost 300 enzymes involved in almost all stages of metabolism. In addition to its role in the enzymatic catalysis and gene expression, zinc stabilizes the structure of proteins and nucleic acids, contributes to preservation of integrity of subcellular organelles, participates in transport processes, and plays an important role in the immune response [1]. Zinc also efficiently forms complexes with oxygen- and nitrogen-containing ligands; therefore, study of the biological properties of zinc complexes is a relevant task.

A weighty factor stimulating active research in this field is the biological activity of the ligands themselves, because the biological properties of coordination compounds depend on not only the nature of the metal, but also the nature of the ligands and functional groups involved in the coordination. In recent years, the tetrazole chemistry has been rapidly developed; hundreds of papers devoted to the synthesis of new functionally substituted derivatives of this class of ligands are published every year [2, 3].

Tetrazoles and their derivatives exhibit antibacterial [4, 5], anti-inflammatory, antifungal [6−9], antiviral [10, 11], anti-tuberculosis, antinociceptive, hypoglycemic, and many other types of activity; they can also act as cyclooxygenase inhibitors and have anti-tumor action [12−16]. In addition, tetrazoles are used as catalysts in the synthesis of phosphonates [17].

Thus, coordination compounds containing tetrazole derivatives can be expected to have a high biological activity. Previously, our research team synthesized and characterized a series of cytotoxic copper(II) complexes based on 5-benzyltetrazole and 2,2'-bipyridine (Bipy) or 1,10-phenanthroline (Phen) derivatives [18]. For further studies of the effect of the central ion on the biological properties of complexes, it was reasonable to obtain related complexes based on 5-benzyltetrazole.

In this study, we prepared a mixed-ligand zinc(II) complex with 5-benzyltetrazole (HL) and 1,10-phenanthroline (Phen) and determined its structure by X-ray diffraction for the first time. The cytotoxic activity of the complex was studied against hepatocellular carcinoma cells (HepG-2) and noncancerous human fibroblasts (MRC-5). The activity of the zinc complex was compared with the activity of analogous mixed-ligand copper(II) complex.

EXPERIMENTAL

Complex **I** was synthesized using commercially available analytical grade zinc(II) acetate and com-

mercially available organic ligands: 5-benzyltetrazole (99% purity) and 1,10-phenanthroline (98% purity).

Synthesis of [Zn(Phen)(H₂O)L₂] (I). A zinc(II) acetate powder (0.10 mmol, 0.022 g) was added to an ethanol solution (2 mL) of Phen (0.10 mmol, 0.019 g), and the resulting colorless solution was magnetically stirred for 5 min. A solution of HL (0.20 mmol, 0.032 g) in ethanol (2 mL) was added to the obtained solution. The resulting solution was filtered through a paper filter (blue ribbon) and left for a long time for crystallization. For several months, the mother liquor was evaporated without crystal formation, then DMSO (3 mL) was added, and the solution was again left for crystallization. Slow crystallization from DMSO in air at room temperature gave single crystals suitable for X-ray diffraction. The crystals were collected on a glass filter and washed with minor portions of ethanol. The yield was 0.030 g (52%).

IR (ν, cm^{-1}): 3200 ν(OH), 3026, 2954, 2920, 2855 ν(CH); 1627, 1609, 1581, 1535, 1517, 1463 (R$_{ring}$).

For C$_{28}$H$_{24}$N$_{10}$OZn

Anal. calcd., %	C, 57.8	H, 4.2	B, 24.1
Found, %	C, 57.4	H, 4.2	B, 23.8

The ^{1}H and ^{13}C NMR signal assignment is depicted in Scheme 1.
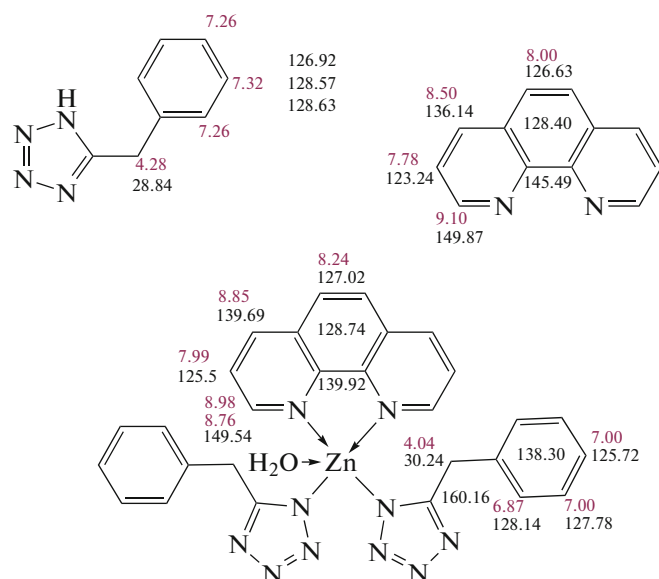
Scheme 1.

^{1}H NMR (δ, ppm): δ 4.04 (br.s, 4H, CH$_2$(HL)), 6.87 (br.s, 4H, o-Ph(HL)), 7.00 (br.s, 6H, m,p-Ph(HL)), 7.99 (br.s, 2H, 3,8-Phen), 8.24 (br.s, 2H, 5,6-Phen), 8.76 (br.s, 1H, 2-Phen), 8.85 (br.s, 2H, 4,7-Phen), 8.98 (br.s, 1H, 10-Phen).

^{13}C NMR (δ, ppm): δ 30.24 (CH$_2$(HL)), 125.50 (3,8-Phen), 125.72 (p-Ph), 127.02 (5,6-Phen), 127.78 (m-Ph), 128.14 (o-Ph), 128.74 (4a,6a-Phen), 138.30 (i-Ph), 139.69 (4,7-Phen), 139.92 (1a,10a-Phen), 149.54 (2,9-Phen), 160.16 (C=N (HL)).

Elemental analysis for C, H, N was carried out at the analytical laboratory of the Nikolaev Institute of Inorganic Chemistry, Siberian Branch, Russian Academy of Sciences, using a Vario MICRO Cube CHNS analyzer by a standard procedure.

IR spectra were measured on a Scimitar FTS 2000 FTIR spectrometer in the 4000–400 cm^{-1} range. The samples were prepared as suspensions in mineral or fluorinated oil.

Powder X-ray diffraction analysis was carried out on a Shimadzu XRD-7000 diffractometer (CuK_α radiation, Ni filter, 2θ range from 5° to 50° with 0.03° step, acquisition of 1 s in each point).

NMR spectra were recorded on a Bruker Avance III 500 spectrometer operating at 499.93 MHz for ^{1}H and at 125.71 MHz for ^{13}C. A saturated solution of complex **I** (10 mM) in DMSO and a 10 mM solution of a mixture of free ligands were used. The experiments were performed at two temperatures: 300 and 323 K. Solvent signals, δ = 2.50 ppm for the residual protons (for ^{1}H NMR spectra) and δ = 39.5 ppm (for ^{13}C NMR spectra) were used as standards.

X-ray diffraction study of complex **I** was carried out on a Bruker D8 Venture diffractometer using a monochromatic graphite MoK_α radiation (λ = 0.71073 Å) at 150 K (Table 1). The absorption corrections were applied using the SADABS program [19]. The structure was solved by direct methods and refined using SHELXTL [20] and OLEX2 (in the graphical inter-

Table 1. Crystallographic data and X-ray experiment and structure refinement details for complex **I**

Parameters	Values
Molecular formula	$C_{28}H_{24}N_{10}OZn$
M	581.94
System	Orthorhombic
Space group	*Pnma*
a, Å	20.9174(5)
b, Å	12.2910(3)
c, Å	10.0573(2)
α, deg	90
β, deg	90
γ, deg	90
V, Å^3	2585.69(10)
Z	4
ρ(calcd.), g/cm^3	1.495
μ, mm^{-1}	0.994
Crystal size, mm	$0.18 \times 0.12 \times 0.05$
Data collection range on 2θ, deg	4.49–63.02
Ranges of h, k, l	$-20 \le h \le 23, -15 \le k \le 13, -40 \le l \le 37$
Number of measured reflections	52077
Number of unique reflections (R_{int}, R_σ)	4479 (0.0482, 0.0234)
Number of refined parameters	209
Number of constraints	0
GOOF on F^2	1.024
R_1, wR_2 ($I > 2\sigma(I)$)	0.0285, 0.0701
R_1, wR_2 (all data)	0.0381, 0.0741
$\Delta\rho_{max}/\Delta\rho_{min}$, e Å^{-3}	0.38/−0.30

face) [21] software. The atomic displacement parameters for nonhydrogen atoms were refined anisotropically. The hydrogen atom positions were calculated geometrically and refined in the riding model.

The full set of the X-ray diffraction data is deposited with the Cambridge Crystallographic Data Centre (CCDC no. 2220597; https://www.ccdc.cam. ac.uk/structures) and is available from the authors.

Cytotoxic activity. Cell viability was evaluated for HepG-2 (hepatocarcinoma) and MRC-5 (noncancerous human fibroblasts) cells, which were cultured in 96-well plates in the IMDM medium in a CO_2 incubator. After 24 h, the DMSO solutions of the agents (in the 1−100 µM concentration range) were added and incubated for 48 h. Then fluorescence dyes, Hoechst 33342 (Sigma-Aldrich) and propidium iodide (Invitrogen), were added and incubated for 30 min. The

measurements were done on an IN Cell Analyzer 2200 (GE Healthcare, UK) in an automated mode of four fields per well. The obtained images were analyzed using the IN Cell Investigator program package. The results was presented as average percentages of living and dead cells and the cells undergoing apoptosis ± standard deviation.

RESULTS AND DISCUSSION

Complex **I** was obtained by slow crystallization from a DMSO solution containing zinc(II) acetate, 5-benzyltetrazole, and 1,10-phenanthroline (Scheme 2). The Zn^{2+} : Phen : HL ratio in the synthesis was 1 : 1 : 2, which made it possible to obtain the pure phase of **I** in a fairly high yield (52%). The product was soluble in DMSO and ethanol and was poorly soluble in acetonitrile, acetone, water, and phosphate buffer.

Scheme 2.
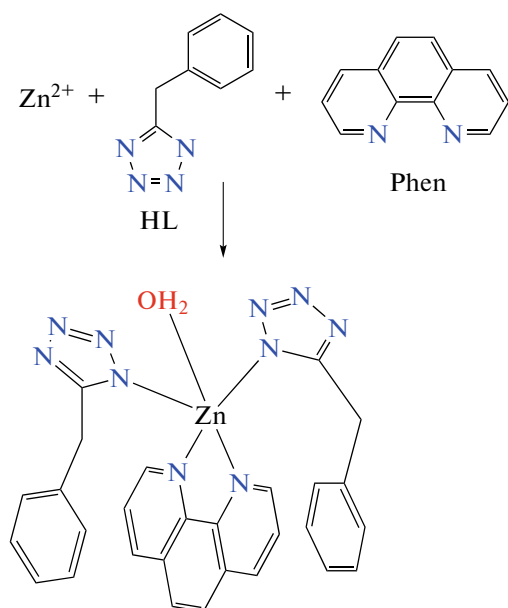
The key characteristic frequencies in the IR spectrum of **I** are presented in Experimental. The 3030–2855 cm^{-1} range contains bands characteristic of ν(C−H) stretching modes of the benzene ring, while the 1630–1463 cm^{-1} range shows stretching vibrations of the aromatic rings of the ligands. In addition, the stretching band of the coordinated water molecule is present (3200 cm^{-1}).

The single crystals were isolated from the mother liquor as colorless plates. According to the X-ray diffraction data, the obtained zinc(II) complex is mononuclear (Fig. 1a). The environment of the central atom comprises four nitrogen atoms and one oxygen atom. Thus, the zinc(II) coordination polyhedron can be described as a trigonal bipyramid, the parameters SHAPE $S(D_{3h})$ and τ_5 are 0.69 and 0.75, which confirms the geometry of the coordination sphere. The Zn−N and Zn−O bond lengths in the equatorial plane vary in the 2.1059(13)−2.1963(14) Å range and the length of the apical Zn−N bond is 2.0113(10) Å. The 5-benzyltetrazolate ion is coordinated only in the monodentate fashion via the N(1) atom of the tetrazole ring. In addition, intramolecular π-stacking (3.700 Å) between the phenyl group of the ligand L$^-$ and 1,10-phenanthroline takes place in the compound. The coordinated water molecule is hydrogen-bonded to the tetrazolate nitrogen atoms of the nearest molecules of the complex; the O···N distance is 2.773 Å. As a result, mononuclear compounds are linked into a polymer chain arranged along the *b* crystallographic axis (Fig. 1b).

Powder X-ray diffraction confirmed the single-phase nature of complex **I** (Fig. 2).

Since the stability of the compound in solution is important for the subsequent cytotoxicity assays, the behavior of complex **I** in a DMSO solution was studied by NMR spectrosopy.

On the basis of ^{1}H NMR spectra alone, it can be stated that complex **I** is stable in solutions. In comparison with the spectrum of a mixture of ligands, in the spectrum of the complex, the signals of all hydrogen atoms of L$^-$ are considerably shifted upfield from 4.28 to 4.04 ppm (Fig. 3c and 3a). Despite the considerable distance from the donor atom, significant differences are still observed for the phenyl hydrogen atoms. Conversely, in the case of Phen, coordination leads to deshielding of the hydrogen nuclei and, consequently, to downfield shifts of the signals. The only exception are the hydrogen atoms in positions 2 and 9, which are shifted by 0.1−0.35 ppm. This difference is apparently associated with the geometry of the complex in solution, in which these hydrogen atoms are located in the shielded region created by the benzene ring of L$^-$ ligand.

Attention is attracted by rather large signal width in the ^{1}H NMR spectrum and also the fact that hydrogen atoms in positions 2 and 9 are nonequivalent in the spectrum (8.76 and 8.98 ppm). This situation can be explained by assuming the stereochemical rigidity of the complex in solutions at room temperature. Indeed, heating of the solution to 323 K results in marked narrowing of the lines (the central spectrum in Fig. 3b) and coalescence of α-proton signals into one signal (8.89 ppm). Despite the considerable heating (in comparison with the physiological temperature), the positions of other signals in the spectrum do not change, which indicates that the complex is stable even under these conditions.

The ^{13}C NMR spectra of complex **I** and free ligands are also considerably different (Fig. 4). The methylene carbon signal is shifted downfield by ~1.5 ppm. A ~1 ppm shift is also observed for carbon signals from the phenyl group. The spectrum of complex **I** shows the carbon signal for the tetrazole ring, which is not manifested in the spectrum of free ligand due to the considerable broadening caused by the presence of active hydrogen atom in the NH group. The Phen signals, similarly to those in the ^{1}H NMR spectrum, are markedly broadened and slightly shifted with respect to these signals of the free ligand. The ^{13}C NMR spectra at elevated temperature have not been recorded due to low solubility of complex **I** and, as a consequence, great duration of the high-temperature experiment.

Thus, it can be concluded that the ^{13}C NMR spectroscopic data are in fully in line with the ^{1}H NMR data. Both ligands occur in the coordinated state throughout the period of the experiment (48 h). Detailed NMR data are shown in Figs. S1−S4.

The effect of the ligands and complex **I** on the viability of human cells was evaluated using the HepG-2 (hepatocellular carcinoma) cells and MRC-5 cells (noncancerous human fibroblasts) and staining with
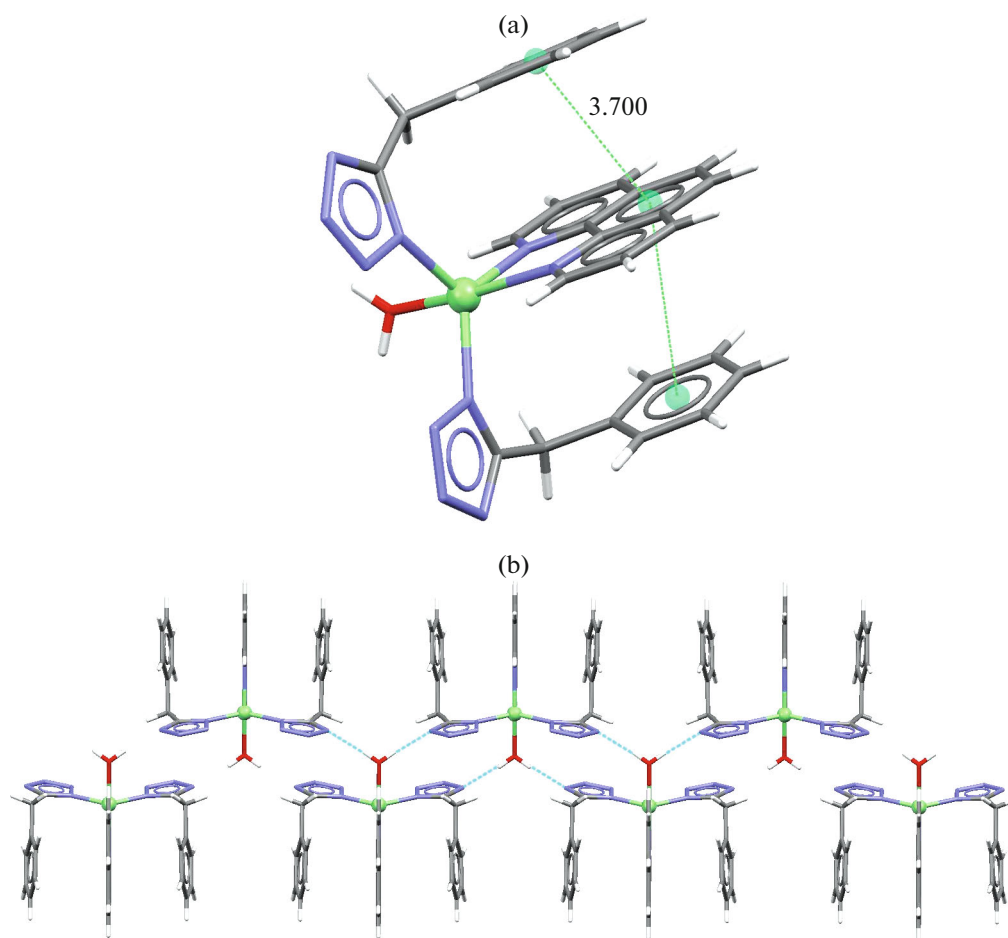
Fig. 1. (a) Structure of complex **I** and (b) polymer chains formed by hydrogen bonds.

Hoechst 33342/propidium iodide fluorescence dyes. The cytotoxic effect was assessed by three parameters: percentages of living cells, dead cells, and apoptotic cells. The agents (zinc(II) acetate, ligands, and complex **I**) were dissolved in an appropriate solvent (water for zinc(II) acetate; ethanol for HL and Phen; and DMSO for complex **I**), diluted with cell medium to specified concentrations, and added to the cells occurring in a nutrition medium in 1−100 μM concentrations. Cisplatin was tested under the same conditions and used for comparison.

No cytotoxicity is observed in the concentration range of 0.1−50 μM (the incubation time with the agents was 48 h) after treatment of the HepG-2 and MRC-5 cells with the initial reagents: $Zn(OAc)_2$, 5-benzyltetrazole, and 1,10-phenanthroline.

The obtained complex **I** shows a slight cytotoxic activity in the concentration range of 1−100 μM; the cell death (10−15%) after treatment with this complex started at 50 μM in the HepG-2 cell line. In addition, pronounced cytostatic activity is present, as shown in Fig. 5a. The amount of cells decreases relative to the control over time, being 40−45% of the control in the case of HepG-2. Complex **I** proved to be less toxic than cisplatin, for which the IC_{50} value (half-maximum inhibitory concentration) against the HepG-2 cell line is 33.0 ± 5.4.

Further, the compound was tested on noncancerous normal human fibroblasts (MRC-5) (Fig. 5b). Like in the case of HepG-2, the percentage of dead cells markedly increases in the concentration range of 1−100 μM; also, clear-cut cytostatic action on this cell line is present: the percentage of living cells is 10−20% relative to the control (starting from the compound concentration of 5 μM). In addition, the percentage of apoptotic cells considerably increases, starting from the compound concentration of 5 μM, and reaches a maximum (~30%) when the concentration is 50 μM. Nevertheless, a 50% cell death is not attained even for 100 μM concentration. Therefore, it is impossible to calculate the IC_{50} value and the selectivity index (the ratio of the IC50 values on MRC-5 to that on the HepG-2 cell line). Cisplatin is nontoxic up to 50 μM against the noncancerous MRC-5 cells.
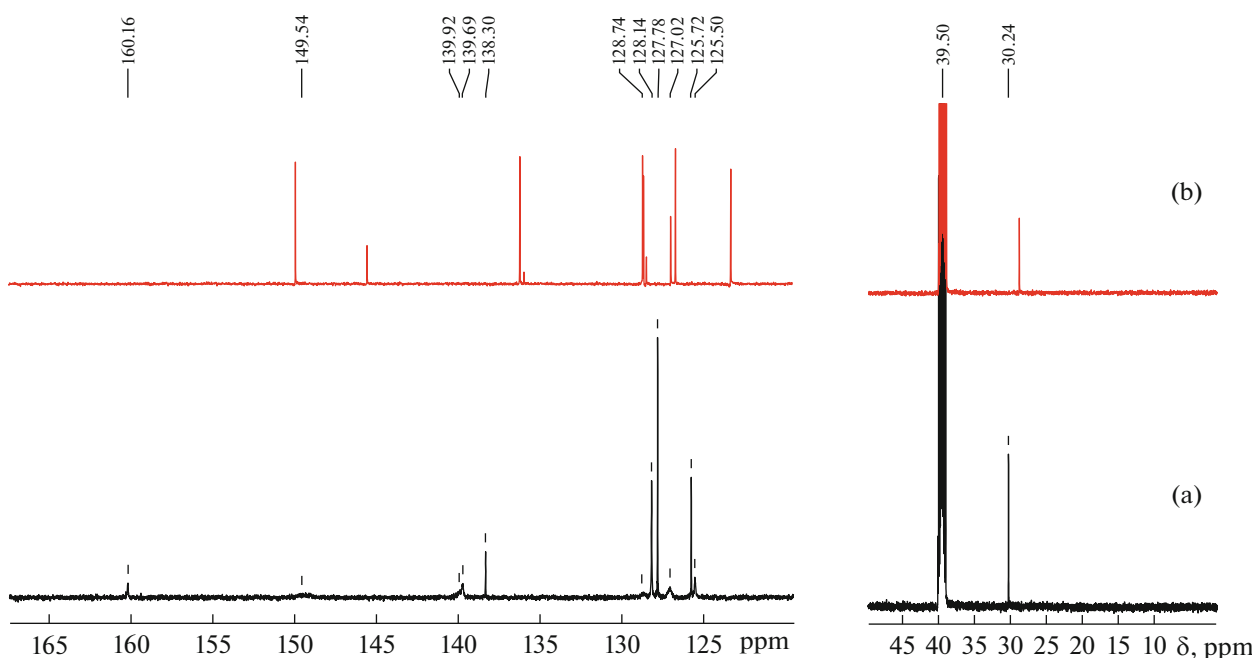
A similar copper(II) complex with HL and Phen showed an obvious dose-dependent cytotoxic activity
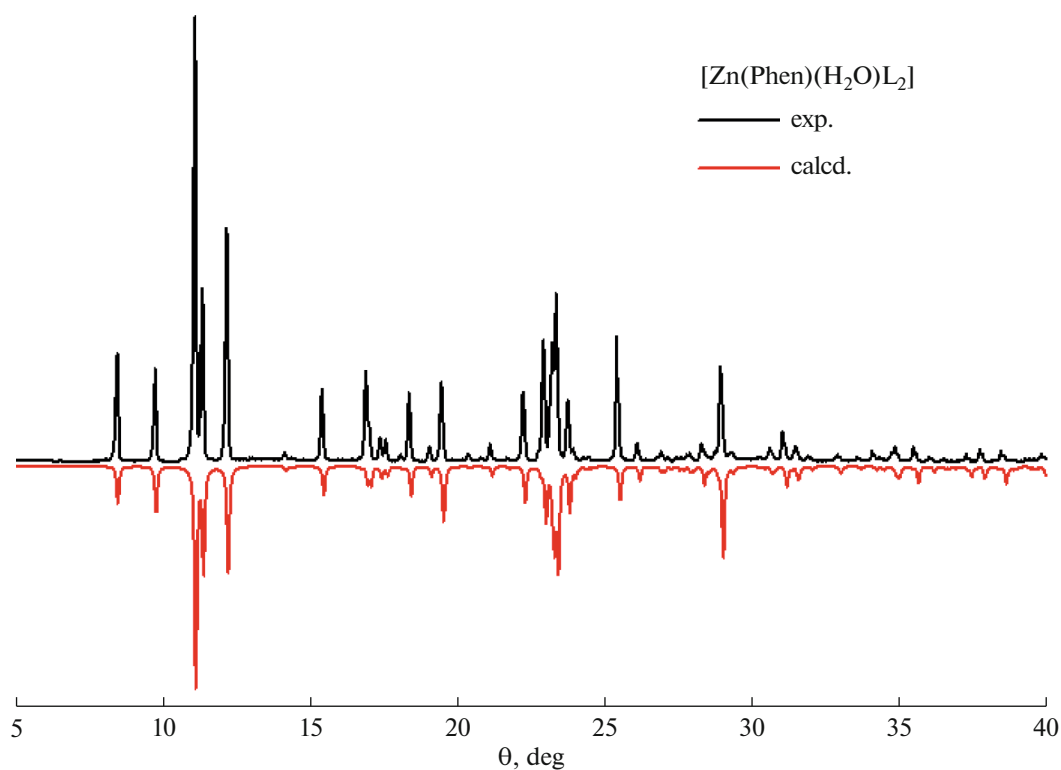
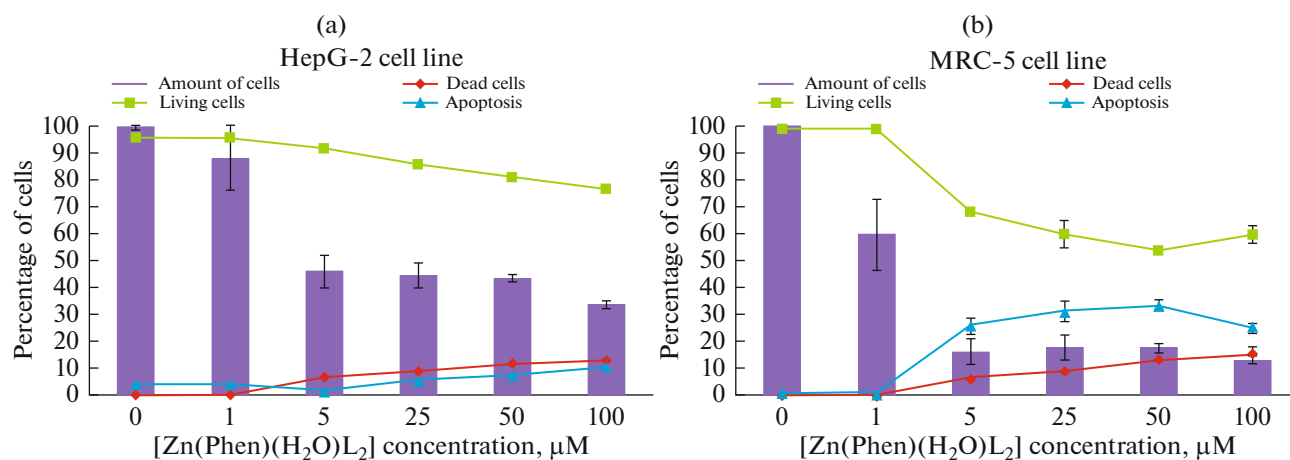**Fig. 2.** X-ray diffraction pattern of complex **I**.
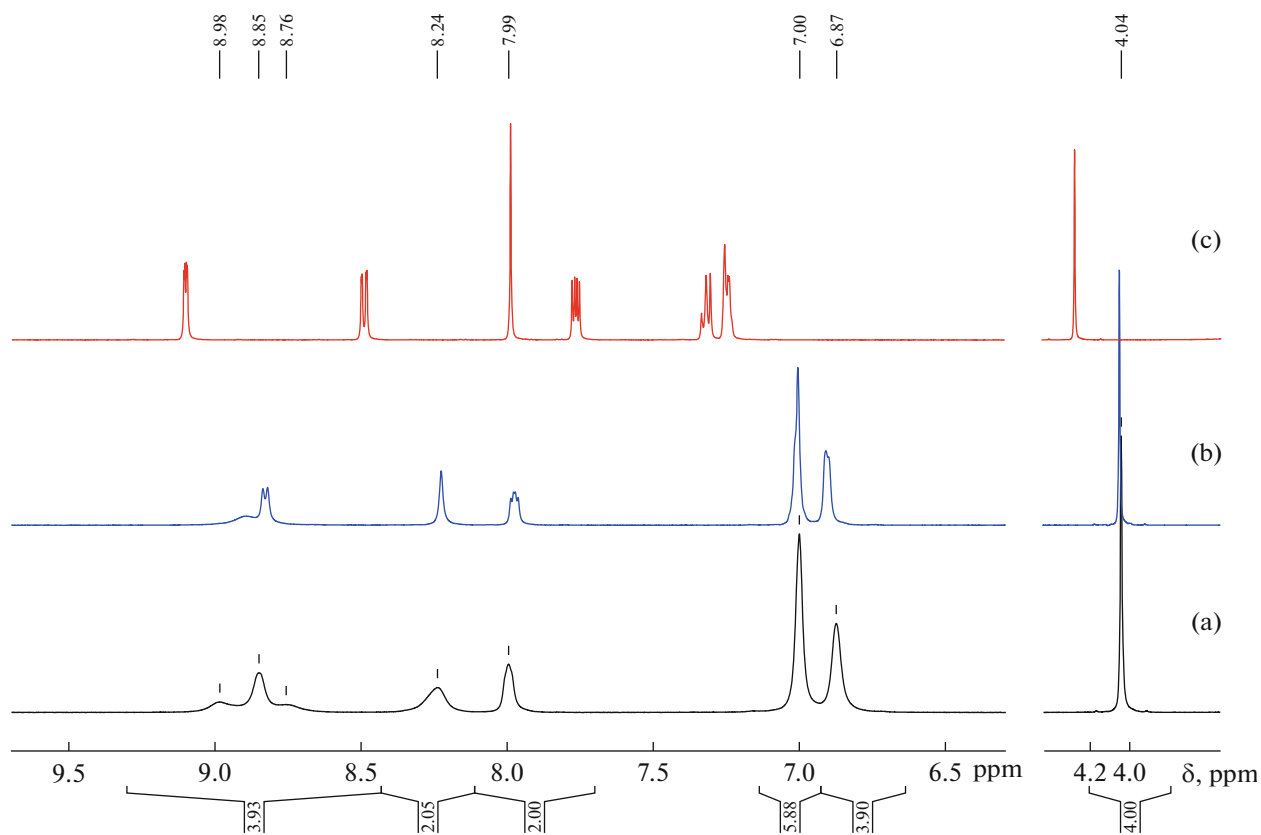
Fig. 3. Comparison of the ^{1}H NMR spectra: (a) solution of complex **I** at room temperature, (b) solution of complex **I** at 323 K, (c) mixture of 10 mM solutions of HL and Phen.

Fig. 4. Comparison of the ^{13}C NMR spectra: (a) solution of complex **I** at room temperature, (b) mixture of 10 mM solutions of HL and Phen.

Fig. 5. Survival rates of (a) HepG-2 and (b) MRC-5 cells for complex **I**.

against the HepG-2 cell line; the IC_{50} value in this case is 6.7 ± 0.3 μM [18]. Thus, this study confirms the assumption that the [Cu(Phen)] moiety plays a key role in the cytotoxic activity and that replacement of the copper ion by the zinc ion decreases the activity.

Thus, we synthesized and characterized the mononuclear zinc(II) complex based on 1,10-phenanthroline and a tetrazole derivative, 5-benzyltetrazole. It was found that the zinc(II) atom in the complex has a coordination environment of a distorted trigonal bipyramid where zinc coordinates two L^- ligands via the tetrazolate nitrogen atoms, one 1,10-phenanthroline molecule, and one water molecule. The stability of the complex in solutions for 48 h was confirmed by NMR spectroscopy; during 48 h, the ligands remain coordinated to the zinc(II) ion. The cytotoxicity assays revealed no significant cytotoxic effect on the HepG-2 hepatocellular carcinoma cell line and MRC-5 noncancerous human fibroblasts (in the 1–100 μM range). Nevertheless, the complex showed cytostatic activity for both cell lines.

The online version contains supplementary material available at https://doi.org/10.1134/S1070328423600158.

CONFLICT OF INTEREST

The authors declare that they have no conflicts of interest.

SUPPLEMENTARY INFORMATION

The online version contains supplementary material available at https://doi.org/10.1134/S1070328423600158.

REFERENCES

1. Vallee, B.L. and Auld, D.S., *Proc. Natl. Acad. Sci. USA*, 1990, vol. 87, no. 1, p. 220.
2. Ostrovskii, V.A., Koldobskii, G.I., and Trifonov, R.E., *Comprehensive Heterocyclic Chemistry III*, Oxford: Elsevier, 2008, p. 259.
3. Ostrovskii, V.A., Trifonov, R.E., and Popova, E.A., *Russ. Chem. Bull.*, 2012, vol. 61, no. 4, p. 768.
4. Dofe, V.S., Sarkate, A.P., Kathwate, S.H., et al., *Heterocycl. Commun.*, 2017, vol. 23, no. 4, p. 325.
5. Chohan, Z.H., Supuran, C.T., and Scozzafava, A., *J. Enzyme Inhib. Med. Chem.*, 2008, vol. 19, no. 1, p. 79.
6. Brand, S.R., Degenhardt, T.P., Person, K., et al., *Am. J. Obstet. Gynecol.*, 2017, vol. 217, no. 6, p. 715.
7. Hoekstra, W.J., Hargrove, T.Y., Wawrzak, Z., et al., *Antimicrob. Agents Chemother.*, 2015, vol. 60, no. 2, p. 1058.
8. Gonzalez-Lara, M.F., Sifuentes-Osornio, J., and Ostrosky-Zeichner, L., *Drugs*, 2017, vol. 77, no. 14, p. 1505.
9. Warrilow, A.G.S., Parker, J.E., Price, C.L., et al., *Antimicrob. Agents Chemother.*, 2016, vol. 60, no. 8, p. 4530.
10. May, B.C.H. and Abell, A.D., *Tetrahedron Lett.*, 2001, vol. 42, no. 33, p. 5641.
11. May, B.C.H. and Abell, A.D., *J. Chem. Soc., Perkin Trans.*, 2002, vol. 2, no. 2, p. 172.
12. Popova, E.A., Protas, A.V., and Trifonov, R.E., *Anticancer. Agents Med. Chem.*, 2017, vol. 17, no. 14, p. 1856.
13. Romagnoli, R., Baraldi, P.G., Salvador, M.K., et al., *J. Med. Chem.*, 2012, vol. 55, no. 1, p. 475.
14. Jedhe, G.S., Paul, D., Gonnade, R.G., et al., *Bioorganic Med. Chem. Lett.*, 2013, vol. 23, no. 16, p. 4680.
15. Beale, T.M., Allwood, D.M., Bender, A., et al., *ACS Med. Chem. Lett.*, 2012, vol. 3, no. 3, p. 177.
16. Subba Rao, A.V., Swapna, K., Shaik, S.P., et al., *Bioorganic Med. Chem.*, 2017, vol. 25, no. 3, p. 977.
17. Mohite, P.B. and Bhaskar, V.H., *Int. J. PharmTech Res.*, 2011, vol. 3, no. 3, p. 1557.
18. Eremina, J.A., Smirnova, K.S., Klyushova, L.S., et al., *J. Mol. Struct.*, 2021, vol. 1245, p. 131024.
19. *Bruker Apex3 Software Suite: Apex3, SADABS-2016/2 and SAINT. Version 2018.7-2*, Madison: Bruker AXS Inc., 2017.
20. Sheldrick, G.M., *Acta Crystallogr., Sect. A: Found. Adv.*, 2015, vol. 71, p. 3.
21. Sheldrick, G.M., *Acta Crystallogr., Sect. C: Struct. Chem.*, 2015, vol. 71, p. 3.

Translated by Z. Svitanko